J Nanopart Res (2020) 22: 109
https://doi.org/10.1007/s11051-020-04831-9

RESEARCH PAPER

Surface-modified polycaprolactone nanoparticles for the brain-targeted delivery of nevirapine

Sunita Lahkar · Malay Kumar Das

Received: 1 October 2019 / Accepted: 30 March 2020 / Published online: 8 May 2020

Abstract The low-density lipoprotein (LDL) receptors overexpressed in brain capillary endothelial cell (BCEC) membrane were successfully targeted by polysorbate 80 (PS80)-coated polycaprolactone (PCL) nanoparticles for brain delivery of nevirapine (NVP). The nanoparticles prepared by emulsion solvent evaporation technique were evaluated for mean particle size (nm), zeta potential (mV), percentage drug entrapment efficiency (% EE), percentage drug loading (% DL), Fourier transform infrared (FT-IR) spectroscopy, differential scanning calorimetry (DSC), scanning electron microscopy (SEM), transmission electron microscopy (TEM), in vitro drug release study, stability study and in vivo biodistribution study. The mean particle size (nm) of uncoated nanoparticles, NvPNPs5, and PS80-coated nanoparticles, P80NvPNPs5, were (128.43 ± 4.82) nm and (218.3 ± 7.3) nm, respectively. The SEM and TEM analysis showed small-sized (< 100 nm), spherical-shaped, smooth-surface nanoparticles with less aggregation. The zeta potential (mV) analysis showed stable nanoparticles with values (− 72.1 ± 0.00) mV, NvPNPs5; (− 16.2 ± 0.00) mV, P80NvPNPs5; (− 16.2 ± 0.00) mV, 6CFNvPNPs5; and (− 13.6 ± 0.00) mV, P806CFNvPNPs5. The FT-IR and DSC report indicated drug excipient compatibility. P80NvPNPs5 showed an *in vitro* drug release for 36 h and its release kinetic was best fitted in Higuchi model ($R^2 = 0.936$). Korsemeyer Peppas model showed an anomalous non-Fickian drug release mechanism as $n = 0.767$. P80NvPNPs5 released NVP for 24 h in the brain with prolonged blood circulation for 48 h as compared with NvPNPs5 and free drug suspension, ($p < 0.05$) in *in vivo* biodistribution study in Swiss Wistar rat. The confocal laser scanning microscopy (CLSM) study showed uniform distribution of P80NvPNPs5 in rat BCECs for 24 h post i.v. administration. The present observation concludes the futuristic scope of P80NvPNPs5 nanoparticles for brain delivery of different antiretroviral drugs as well as other CNS active drugs to treat several CNS disorders.

Keywords Blood-brain barrier · Polycaprolactone nanoparticles · Nevirapine · Polysorbate 80 · Brain-targeted drug delivery · Nanomedicine

S. Lahkar (✉) · M. K. Das
Department of Pharmaceutical Sciences, Dibrugarh University, Dibrugarh, Assam, India
e-mail: sunitalahkar@gmail.com

Introduction

Acquired immunodeficiency syndrome (AIDS) caused by the human immunodeficiency virus (HIV) is responsible for the death of millions of people. WHO reported the existence of 36.7 million HIV-infected people worldwide in 2016, out of which 1 million people died of HIV-related illness worldwide in 2016 (Sabin and Lundgren 2013). One such HIV-related illness known as neurological disorders occurs, when the HIV infection penetrates the brain. Initial stage causes mild unrecognizable disease known as HIV-associated neurocognitive disorders (HAND). It is reported that, in 1980, half of the HIV-infected population suffered

from HIV-associated dementia (HAD), AIDS dementia complex (ADC), progressive multifocal toxoplasmosis, cryptococcal meningitis, leukoencephalopathy and peripheral neuropathy due to damage of nerves (Tan and McArthur 2012; Patil and Patil 2014). Till date, available conventional treatment known as highly active antiretroviral therapy (HAART) (Saksena and Smit 2005) fails to treat the HIV-related brain disorders. The blood-brain barrier (BBB) is the major hindrance inhibiting the penetration of HAART into the brain parenchyma. The blood-brain barrier is composed of tight junction of brain capillary endothelial cells (BCECs) and efflux transport which regulate the exchange of nutrients or bioactive substances between the peripheral blood capillaries and the central nervous system (CNS) (Daneman and Prat 2015; Wong et al. 2013). Only the lipophilic drugs, small-sized molecules of molecular weight lesser than 500 Da, can penetrate through the blood-brain barrier while hydrophilic drugs fail (Pardridge 2005). To solve these problems, several strategies have been developed that mimic the endogenous transport system. Among the several types of endogenous transport system, receptor-mediated transport (RMT) is an attractive approach. There are receptors present in the blood-brain barrier like insulin, leptin, insulin-like growth factor, transferrin; LDL (Lajoie and Shusta 2015). Among these, mimicking the LDL receptor expressed on the luminal membrane of BCECs gives a good platform for brain-targeted delivery. Brain targeting using nanoparticles based on passive diffusion is one such non-invasive strategy (Acharya and Reddy 2016). Among the different types of nanoparticles, polymeric nanoparticles are one of the better choices for brain-targeted delivery (Saraiva et al. 2016). The requisite factors for brain-targeted delivery using polymeric nanoparticles are, firstly, the nanoparticles should be small sized. Secondly, avoidance of phagocytosis by the reticuloendothelial system (RES), mononuclear phagocytosis (MPS), liver and splenic filtration. Thirdly, surface modification of the nanoparticles (Storm et al. 1995). The surface modification is required to avoid the adsorption of serum protein, opsonin such as immunoglobulin, complement product C3b and fibronectin (Salmaso and Caliceti 2013). When opsonin gets adsorbed on the surface causes rapid clearance and phagocytosis by the reticuloendothelial cells (RES) in blood, mononuclear phagocytosis system (MPS) organs—liver and spleen. It reduces the half-life of the drug and consequently, insufficient drug can reach and interact with the BCECs, across the blood-brain barrier. Thus, it is necessary to modify the surface of nanoparticles so as to avoid opsonization and engulfment by MPS (Choi et al. 2003). It is reported that the surface modification can be done by coating with a nonionic surfactant like PS80 (Yadav et al. 2017). PS80-coated polymeric nanoparticles recognize LDL receptors in the luminal membrane of the blood-brain barrier and penetrate the BCECs by receptor-mediated endocytosis (RMT) (Sun et al. 2004; Tian et al. 2011). In our present work, effort has been made to target NVP to brain by loading in polymeric nanoparticles. NVP belongs to non-nucleoside reverse transcriptase inhibitor, a Biopharmaceutics classification (BCS) class II drug. It is used in HAART either alone or in combination with other antiretroviral drugs (Indian Pharmacopoeia, 2007). Its poor aqueous solubility causes poor drug release at targeted site. Except these, it suffers from several drawbacks such as long-term therapy, liver toxicity, patient incompliance, frequent dosing, hepatotoxicity, nonspecific targeting on oral administration, first-pass metabolism, enzymatic degradation etc. (Usach et al. 2013). Ultimately, concentration of NVP reaching blood-brain barrier becomes lesser than optimum therapeutic concentration and hence suffers from poor bioavailability in brain. Till date, NVP-related drawbacks in HAART are overcome by incorporating NVP in polymeric nanoparticles. One such nanocarrier is poly lactide-co-glycolide (PLGA) nanoparticles grafted with transferrin (TfR). A successful delivery of NVP across human brain microvascular endothelial cells (HBMECs) when loaded in TfR-grafted PLGA nanoparticles is reported (Kuo et al. 2011). However, PLGA suffers from some drawbacks as it has fast degradation and its degradation products, lactic acid (pKa = 3.08) and glycolic acid (pKa = 3.83) makes the medium highly acidic (Ramanujam et al. 2018; Badri et al. 2017). In order to overcome these drawbacks, in our research work, PCL, a US-FDA-approved polymer is used for preparing polymeric nanoparticles. PCL may offer benefits as it is biocompatible, biodegradable. Moreover, it is suitable for sustained release formulation as it degrades slowly due to its degradation period of 2–3 years. Also, it undergoes lower acidity of its degradation product, caproic acid (pKa = 4.84) (Azimi et al. 2014). As it was discussed previously, NVP-loaded PCL nanoparticles (NvPNPs) could fulfil the required physicochemical characterizations suitable for brain targeting (Lahkar and Das 2017). Thus, the objective of our present work

is to study the potential of PS80-coated PCL nanoparticles as a carrier, for improving bioavailability and sustained release of NVP in brain. The NvPNP nanoparticles were prepared by emulsion solvent evaporation technique (Lahkar and Das 2017). Based on the physicochemical characterizations, optimized nanoformulation was selected for surface coating with PS80 (Ku et al. 2010). Then, PS80-coated NVP-loaded optimized PCL nanoformulation (P80NvPNPs) were compared with uncoated optimized nanoformulation and free drug suspension, in terms of physicochemical characterizations, morphology and surface characteristics, in vitro drug release. The potential of P80NvPNPs in targeting NVP to brain were evaluated by in vivo biodistribution study and CLSM.

Materials and methods

Materials

6-carboxyfluorescein (6CF) and PCL were purchased from Sigma-Aldrich (USA), NVP (pure drug) was purchased from Boehringer Ingelheim (Germany) and pluronic F68 was purchased from Thermo Fisher Scientific (USA). All other chemicals were of analytical grades.

Methods

Preparation of nanoparticles

Preparation and optimization of nanoparticles Initially, for optimization of composition, different nanoformulations were prepared by varying composition of drug:polymer ratio, concentration of poloxamer 188 or pluronic F68 and organic solvent:aqueous phase ratio as shown in Table 1. The nanoformulations were prepared by emulsion solvent evaporation technique at room temperature (25 ± 2 °C) (Lahkar and Das 2017; Pal et al. 2011). As shown in Table 1, the required quantity of organic phase (ethyl acetate) containing PCL and NVP was added dropwise into the aqueous phase containing pluronic F68 and kept under magnetic stirring at 200–300 rpm for 3–5 min. Then the mixture was homogeinized at 20,000 rpm, 20 min using a high-speed homogenizer (Model T25, IKA Ltd., Bangalore, India) followed by ultrasonication (25 °C, 40 KHz) for 20 min using a bath sonicator (UCB320, Spectralab, Mumbai, India) (Lahkar and Das 2017). As ethyl acetate is volatile (boiling point 77.1 °C), so no heat was applied for solvent evaporation. So, the solvent was evaporated by keeping nanosuspension under magnetic stirring at 200–300 rpm for 8–12 h, at room temperature (25 ± 2 °C). Then, the formulation was centrifuged at 15,000 rpm for 20 min; the sediment was collected, washed with distilled water, prefrozen at − 30 °C for 24 h, lyophilized (4.5 Plus freezone, Labanco, USA) at − 30 °C and 180–200 mmHg for 48–72 h and then stored at 4 to 8 °C for further use. The prepared nanoformulations were optimized by the physicochemical characteristics and the optimized composition was selected for further process.

Preparation of PS80-coated nanoparticles The preparation method was same as discussed above, except that 1 ml of 1% w/v of PS80 was added to the optimized nanoformulation during ultrasonication followed by incubation 8–12 h under magnetic stirring at 200–300 rpm for the complete evaporation of the organic solvent. The formulation was centrifuged at 15,000 rpm for 20 min; the sediment was collected, washed with distilled water, prefreezed at − 30 °C for 24 h, lyophilized (4.5 Plus freezone, Labanco, USA) at − 30 °C and 180–200 mmHg for 48–72 h and then stored at 4 to 8 °C for further use.

Preparation of 6CF-tagged nanoparticles The preparation procedure was same above except that 1 ml of 0.16% m/v of 6CF was added to the organic phase of the optimized formulation and incubated for 30 min; before the primary emulsification process. The similar process followed for 6CF-tagged PS80-coated nanoformulation.

Physicochemical characterizations

Determination of particle size The mean particle size and polydispersity index (PDI) of different compositions were determined for optimization. Particle size analyser (Brookhaven 90 plus, New York, USA) based on dynamic laser scattering technique was used to determine mean particle size and polydispersity index (PDI) of optimized nanoparticles, PS80-coated optimized nanoparticles, 6CF-tagged nanoparticles using distilled water as a medium, at room temperature (25 ± 2 °C).

Table 1 Composition for nanoparticles preparation

Excipients	Composition		
	Minimum	Intermediate	Maximum
Drug:polymer ratio	1:4	1:2	1:1
Concentration of poloxamer 188 or pluronic F68	0.5%	1%	2%
Organic solvent:aqueous phase ratio	3:7	4:6	1:1

Determination of % EE and % DL The % EE and % DL were determined by Centrifugation method (Dora et al. 2010). The nanoformulation was centrifuged at 20,000 rpm for 15 min at (25 ± 2 °C). The supernatant was collected and the quantity of unentrapped drug was determined using Ultraviolet-Visible Spectrophotometer (Shimadzu UV 1800, Japan) at 214 nm after suitable dilution. The % EE and % DL was determined using the following relationship (Eqs. 1 and 2) (Lahkar and Das 2017):

$$\%\mathrm{EE} = (\text{Practical Drug Content}/\text{Theoretical Drug Content}) \times 100 \quad (1)$$

$$\%\mathrm{DL} = (\text{Practical Drug Content}/\text{Mass of nanoparticles recover}) \times 10 \quad (2)$$

Determination of zeta potential The Zeta potential of optimized nanoparticles, PS80-coated optimized nanoformulation and 6CF-tagged optimized nanoformulation was determined by laser Doppler microelectrophoresis technique using Zetasizer (Nanoseries ZS90, Malvern Panalytical Ltd., UK) after dilution (1:100) with distilled water, at room temperature (25 ± 2 °C).

Drug excipients compatibility study

FT-IR The FT-IR of NVP, PS80, physical mixture, optimized nanoformulation, PS80-coated optimized nanoformulation, 6CF, 6CF-tagged optimized nanoformulation and 6CF-tagged PS80-coated optimized nanoformulation were carried out using FT-IR spectrophotometer (Bruker Alpha IR, Bruker, USA) in the mid-IR region (wavenumber from 600 cm^{-1} to 4000 cm^{-1}), at room temperature (25 ± 2 °C).

DSC The DSC of NVP, optimized nanoformulation and PS80-coated optimized nanoformulation were carried out using Differential scanning calorimeter (DSC 4000, Perkin Elmer, UK) with the N_2 purge gas flow rate of 20 ml min^{-1} and heat flow rate at 10 °C in^{-1}, at room temperature (25 ± 2 °C).

Morphology and surface characteristics

SEM SEM JSM-6360 (JEOL, Japan) was used to examine the shape and surface morphology of optimized nanoformulation. The nanoparticles were previously coated with a thin layer of gold under vacuum so as to make them electrically conductive. The surface morphology was examined by photomicrographs at an excitation voltage of 20 kV under different magnification.

TEM The shape of optimized nanoformulation and PS80-coated optimized nanoformulation were examined using TEM-JEM 2100 (JEOL, Japan). The diluted nanoparticles were deposited on a copper grid coated with thin carbon film. Then, the nanoparticles were photomicrographed at magnification of 60,000× and 40,000× (Lahkar and Das 2017).

Determination of the binding ratio of fluorescence marker/nevirapine

The unbound fluorescence markers (6CF) and the unbound NVP were determined at room temperature (25 ± 2 °C). 5 ml of the freshly prepared nanosuspension was mixed with 5 ml of distilled water. The nanosuspension was concentrated by centrifugation at 15,000 rpm for 15 min. The supernatant fluid was collected and the amount of 6CF, NVP in the supernatant was quantified by Ultraviolet-Visible spectrophotometer. Thus, the difference in the amount of fluorescence marker or NVP originally employed in the manufacturing process and the amount of unbound fluorescence marker or NVP in

the filtrate gives the quantity of fluorescence marker or NVP bound to the nanoparticles (Reimold et al. 2008).

In vitro drug release study

The in vitro drug release study of optimized nanoformulation, PS80-coated optimized nanoformulation and free drug suspension was determined by Dialysis diffusion bag technique in triplicate ($n = 3$) at room temperature, (25 ± 2 °C) and all parameters of the dissolution apparatus were fixed as per United State Pharmacopoeia (USP) (Souza 2014; Banker and Anderson 1990). Before commencement of the experiment, Phosphate buffer, pH 7.4 was prepared by dissolving, 8 g of sodium chloride (molecular weight 58.4 g/mol), 200 mg potassium chloride (molecular weight 74.551 g/mol), 1.44 g disodium hydrogen phosphate (molecular weight 141.96 g/mol) and 240 mg potassium dihydrogen phosphate (molecular weight 136.086 g/mol) in 800 ml of distilled water. This solution was adjusted to desired pH 7.4 using hydrochloric acid or sodium hydroxide and final volume was adjusted to 1000 ml (Indian Pharmacopoeia, 1996). Here, phosphate buffer, pH 7.4, was used as the dissolution medium, because it resembles human blood pH (7.35–7.45) and the prepared nanoformulation was meant for intravenous administration. The lyophilized nanoparticles (equivalent to 3 mg of drug) were dispersed in 5 ml of phosphate buffer, pH 7.4, in a dialysis membrane bag, tied to the paddle of USP dissolution apparatus II (TDT-08L, Electrolab Dissolution Tester, Mumbai, India) containing 900 ml of Phosphate buffer, pH 7.4 in the presence of a cosolvent (50% *v*/v PEG 4000), at 100 rpm. The temperature of the USP dissolution apparatus II was maintained at (37 ± 0.5 °C) because in vitro drug release / dissolution testing study correlates with human body which is essential to optimize the therapeutic concentration of drug at the site of action. At preset time interval (0.5 h, 1 h, 2 h, 4 h, 6 h, 8 h, 10 h, 12 h, 24 h and 36 h), 10 ml of sample was withdrawn and was replaced with fresh Phosphate buffer pH 7.4. The withdrawn samples were filtered through a membrane filter (0.45 μm, Polytetraflouroethylene, Rankem syringe filter, Rankem chemicals, Haryana, India). One millilitre of this sample was diluted to 10 ml with distilled water and drug content was determined spectrophotometrically at 214 nm using a UV-Visible spectrophotometer (Specord 50 Plus, Analytica Zena, India). The cumulative percent drug release (% CDR) was plotted against different time period ($y = 0.015x + 0.008$, $R^2 = 0.994$) (Lahkar and Das 2017). The dissolution profiles of different kinetic models were compared by inserting in vitro release data in different release kinetic models - Zero order, First order, Higuchi and Hixson-Crowell. 60% of the in vitro release data were fitted in Korsemeyer-Peppas kinetic model to analyse the drug release mechanism using the following relationship (Eq. 3) (Dash et al. 2010).

$$\log(m_t/m_\infty) = \log K + n.\log t \quad (3)$$

where

m_t amount of drug released at time t
m_∞ amount of drug released at infinite time t
K release rate constant
n release exponent (drug release mechanism)

Animal study

Healthy adult male Swiss Wistar rats 150–200 g were purchased from M/S Chakraborty Enterprise, Kolkata (Regd. No. 1433/TO/11/CPCSEA). All the animals were treated according to the standard guidelines compiled by CPCSEA (Committee for the purpose of control and supervision of Experiments on animals, Ministry of Fisheries, Animal Husbandry and Dairying, Govt. of India) after getting approval from Institutional Animal Ethics Committee (IAEC) (No. 1576/GO/a/11/CPCSEA) vide approval number IAEC/DU/79 dated 27/03/2015. The animal house was well ventilated and the animals were maintained on a 12:12 h light/dark cycle. The temperature and relative humidity were maintained at (25 ± 2 °C) and 40–60%, respectively. They were given free access to food and water. Every effort was made to minimize animal suffering and the number of animals used.

In vivo biodistribution study Healthy adult male Swiss Wistar rats 150–200 g were divided into four groups with five rats in each group. The experiment was carried out in triplicate ($n = 3$). The lyophillized nanoparticles were reconstituited in normal saline and filtered through membrane filter (0.22 μm, polytetraflouroethylene, Rankem syringe filter, Rankem chemicals, Haryana, India). Then, the first group was for control. The second group was administered 1.0 ml of NVP suspension (equivalent to 20 mg of NVP/Kg of body weight) in normal saline. The third group was administered 1.0 ml

injection of the optimized lyophilized nanoformulation (equivalent to 20 mg of NVP/Kg of body weight) in the tail vein and the fourth group was administered 1.0 ml injection of the PS80-coated optimized nanoformulation (equivalent to 20 mg of NVP/Kg of body weight). At a time interval of 1 h, 2 h, 4 h, 6 h and 24 h, blood were drawn from the hearts of the rats by inserting syringe needle in the chest of the rat and collected in ice cooled Heparin tubes. The collected blood was immediately centrifuged at 5000 rpm for 15 min to separate plasma. This plasma was stored at − 80 °C until further use. After collecting the blood, the animals were sacrificed and the skull of the animals was cut open, the brain was collected, immediately weighed and stored in 15 ml centrifuge tubes at − 80 °C until further use (Jia et al. 2016). To the 100 μL of collected plasma, 1 ml of Acetonitrile was added, mixed well and kept for 30 min at room temperature. The mixture was centrifuged at 13000 rpm, the supernatant was collected. Another 1 ml of Acetonitrile was added and the same steps were followed twice. Finally, the collected 3 ml of the supernatant was mixed together and dried completely at 45 °C in a hot air oven (Bondi et al. 2010). The brain was homogenized in a tissue homogenizer (RQT-127 A/D, Remi laboratory homogenizer, India) at 2000 rpm with 10 ml of distilled water. The mixture was kept aside for some time. One hundred microlitres of the supernatant was collected and procedures as discussed for blood plasma were followed. Similar procedures (as discussed for blood plasma and brain) were followed for liver, spleen and kidney. The quantitative determination of the drug was done by HPLC (HPLC 1200 series, Agilent technology, USA) with reference to Indian Pharmacopoeia 2007. The dried content was dissolved in HPLC mobile phase consisting of 20 volume of Methanol, 20 volume of Acetonitrile and 60 volume of buffer (1.2% w/v sodium dihydrogen phosphate in HPLC water, pH 3). Twenty microlitres was injected into the HPLC column, C18 at a flow rate of 1.2 ml/min and maximum wavelength at 230 nm. The concentration of drug was obtained from the HPLC calibration plot of NVP. For calibration plot of NVP, stock solution (10 μg/ml) was prepared in HPLC mobile phase. Then, serial dilution with HPLC mobile phase was done to get concentrations of 1 μg/ml, 2 μg/ml, 4 μg/ml, 6 μg/ml and 8 μg/ml. Then, 20 μL was injected into the HPLC (similar parameters as discussed) to obtain data for calibration plot. The validation of HPLC procedure was determined according to the International Conference on Harmonization (ICH) guidelines for analytical method validation. So, the linearity was obtained from the calibration plot using least square regression analysis. The specificity of HPLC procedure was measured by comparing the chromatogram of NVP with that obtained from blank blood plasma and brain tissues to detect the presence of any interfering peaks. The precision of the method was determined by repeatibility (intraday precision) and interday precision. Intraday precision was obtained by analysing NVP content in blood plasma in triplicate ($n = 3$) which was repeated for 3 days (interday precision). Similarly, intraday and interday precision was determined for standard solution of NVP (8 μg/ml). Recovery test was performed to determine the accuracy of the HPLC method. Known concentration of NVP solution (1 μg/ml, 4 μg/ml and 8 μg/ml) were spiked into blank samples of blood plasma and brain tissues, followed by HPLC method of analysis (procedure as discussed). The peak area was compared with that of NVP chromatogram and the drug concentration was obtained from the calibration curve (discussed above). This procedure was done in triplicate ($n = 3$). The accuracy test was expressed as percent recovery (mean ± % RSD, $n = 3$) where % RSD denotes '% relative standard deviation'. The Limit of Detection (LOD) and Limit of Quantification (LOQ) were determined from the calibration plot. LOD and LOQ were used to measure the sensitivity of the method (Ravisankar et al. 2015).

Pharmacokinetic analysis The Pharmacokinetic parameters were determined using PK solver software. The data were expressed as mean ± SD ($n = 3$). Statistical analysis was carried out by one way ANOVA, Tukey's test to compare two or more groups using Minitab 18 statistical software, STAT College, PA, USA. The level of significance was set at $p < 0.05$ with a confidence limit of 95% (Ghaly and Sastre 2014).

CLSM The animals were divided into three groups and each group contained five rats. Lyophilized nanoparticles were reconstituted in phosphate buffer saline (PBS, pH 7.4) and filtered through membrane filter (0.22 μm, polytetraflouroethylene, Rankem syringe filter, Rankem chemicals, Haryana, India) before administration. The first group was administered 1.0 ml of 0.16% m/v solution of fluorescence marker 6CF in PBS, pH 7.4 in the tail vein. The second group was administered an injection of 1.0 ml of the 6CF-tagged optimized

nanoformulation (equivalent to 20 mg of NVP/Kg of body weight) in PBS in the tail vein. The third group received an injection of 1.0 ml of the 6CF-tagged PS80-coated optimized nanoformulation (equivalent to 20 mg of NVP / Kg of body weight) in PBS, in the tail vein. The rats were sacrificed by cervical dislocation method at a different time interval of 30 min, 1 h, 2 h, 4 h, 6 h and 24 h. The brain was collected, washed with PBS, immediately embedded in PBS and stored at − 80 °C for further use (Kaur et al. 2008; Hague et al. 2014).

Preparation of cryosectioned slide for CLSM Serial sections (6-μm thickness) were cut using a semi-automated cryotome (Thermo Shandon UK, Model 620E) at − 40 °C and thaw-mounted onto glass slides (Bohn et al. 2016). Brain tissues staining were done with DAPI (1 μg/ml). Brain slides were treated with one drop glycerol and were observed in a CLSM (Leica/TCS SP8, Leica Microsystems, Germany) at 10× magnification. The 6CF-tagged nanoformulation (coated) emitted green fluorescence as observed at 495 nm $_{excitation}$/ 517 nm $_{emission}$. The DAPI stained cells emitted blue fluorescence which was observed at 358 nm $_{excitation}$/ 461 nm $_{emission}$.

Stability studies

The freshly prepared optimized nanoformulation and PS80-coated optimized nanoformulation were divided into two groups ($n = 3$) and stored at refrigerated (5 ± 3 °C) and room temperature (25 ± 2 °C) for 120 days. The physicochemical characterizations were measured at both temperature at different time intervals of 0 days, 30 days, 60 days, 90 days and 120 days (Campos et al. 2015).

Results and discussion

Physicochemical characterizations

Determination of particle size

The composition and physicochemical characteristics of different nanoformulation are given in Table 2. The composition of the optimized nanoformulation, NvPNPs5, was 1:4 (drug:polymer ratio), 1% w/v (concentration of surfactant or pluronic F68) and 3:7 (organic solvent:aqueous phase ratio). The physicochemical characterization showed that mean particle size obtained for NvPNPs5, (128.43 ± 4.82) nm, was smaller as compared with other formulations. NvPNPs5 mean particle size was suitable for brain-targeted delivery. The presence of PS80-coated layer on the surface of P80NvPNPs5, showed a bigger mean particle size, (218.3 ± 7.3) nm than uncoated nanoparticles (Table 3, Fig. 1 (1)) (Chacko et al. 2018). The NvPNPs5 and P80NvPNPs5 when tagged with 6CF, i.e. 6CFNvPNPs5 (optimized) and 6CFP80NvPNPs5 (coated) showed an increase in mean particle size to (187.5 ± 2.35) nm and (259.9 ± 5.05) nm respectively (Table 3).

Determination of % EE and % DL

% EE of NvPNPs5 was lesser than that of other formulations due to its smaller mean particle size (Table 2). During preparation, application of high-speed homogenization and ultrasonication increased the surface area which caused leakage of drug into the surrounding fluid leading to less % EE (Lahkar and Das 2018). Table 3 indicates no change in the % EE and % DL of P80NvPNPs5 as it showed similar % EE and % DL of (39.21 ± 0.05) % and (0.975 ± 0.01) % respectively as that of NvPNPs5. Similarly, 6CFNvPNPs5 and P806CFNvPNPs5 showed similar % EE and % DL as that of NvPNPs5 indicating that the drug remained intact in the nanoparticles.

Determination of zeta potential

The Zeta potential of NvPNPs5, P80NvPNPs5, 6CF-tagged NvPNPs5, 6CFNvPNPs5 and 6CF-tagged PS80-coated optimized nanoformulation, 6CFP80NvPNPs5 indicates high stability of nanoformulations without flocculation in the nanosuspension (Table 3, Fig. 1 (2)). NvPNPs5 (optimized) got a high negative zeta potential value, (− 72.1 ± 0.00) mV. P80NvPNPs5 (coated) showed a lower negative zeta potential value, (− 16.2 ± 0.00) mV. Similarly, the zeta potential value for 6CFNvPNPs5 and 6CFP80NvPNPs5 were (− 16.2 ± 0.00) mV and (− 13.6 ± 0.00) mV, respectively. Although the obtained zeta potential were towards the negative side, it supported the hypothesis that overall, at the local microenvironment surrounding each coated nanoparticles, the net electrical charge would be positive which facilitates the binding of coated nanoparticles to the negatively charged residues on the endothelial cells of the blood-brain barrier. Therefore, it could be assumed that due to relatively less negative

Table 2 Physicochemical characterization and optimization of the formulation

Sr. no.	Drug:polymer ratio	Concentration of surfactant(% w/v)	Organic solvent:aqueous phase ratio	Mean particle size(in nm)	% drug entrapment efficiency(% EE)	% drug loading(% DL)
NvPNPs1	1:4	0.5	4:6	353.75	50.71	0.57
NvPNPs2	1:1	0.5	4:6	273.75	45.62	0.46
NvPNPs3	1:4	2	4:6	276.25	45.81	0.49
NvPNPs4	1:1	2	4:6	366.25	50.99	0.55
NvPNPs5	*1:4*	*1*	*3:7*	*123.2*	*39.21*	*0.975*
NvPNPs6	1:1	1	3:7	129.4	25.81	0.258
NvPNPs7	1:4	1	1:1	251.25	41.32	0.413
NvPNPs8	1:1	1	1:1	281.25	46.72	0.471
NvPNPs9	1:2	0.5	3:7	132.7	33.22	0.37 1
NvPNPs10	1:2	2	3:7	185.1	36.91	0.331
NvPNPs11	1:2	0.5	1:1	265	42.41	0.424
NvPNPs12	1:2	2	1:1	312.5	49.51	0.491
NvPNPs13	1:2	1	4:6	310	48.11	0.482

NvPNPs5 was the optimised nanoformulation and its composition was used for further study

surface charge of coated nanoparticles, it was attracted and adsorbed to the blood-brain barrier endothelial cells and thus enhanced the possibility of NVP delivery to the brain (Chacko et al. 2018; Honary and Zahir 2013; Parikh et al. 2010).

Drug excipients compatibility studies

FT-IR

NVP showed peaks at 3183.27 cm^{-1} (alcohol/phenol, –OH stretching band), 1642.26 cm^{-1} (aromatic C=C bending, amide C=O stretching band), 1381.55 cm^{-1} (alkane, CH stretching band), while PS80 shows peaks at 3284.54 cm^{-1} (alcohol/phenol, –OH stretching band), 1734.55 cm^{-1} (Ketone, C=O stretching band), 1349.29 cm^{-1} (alcohol, OH stretching band) and 1094.34 cm^{-1} (C=O stretching band). Similar functional groups were observed for the physical mixture, NvPNPs5 and P80NvPNPs5 nanoparticles. The result showed successful drug entrapment and surface coating of nanoparticles with PS80 as well as the absence of drug excipient interaction. It showed the compatibility of PS80 with other excipients. The P80NvPNPs5 nanoparticles showed similar functional groups as that of NVP at 3333.20 cm^{-1} (alkane, CH stretch band), 1637.52 cm^{-1} (aromatic C=C bending, amide C=O stretching band) (Fig. 2a). Moreover, 6CF showed the presence of functional groups at 3321.17 cm^{-1} (Alcohol /Phenol -OH stretching band), 2972.97 cm^{-1} (carboxylic acid,-OH stretching band), 1452.96 cm^{-1} (aromatic C=C bending), 1087.43 cm^{-1}, 1045.16 cm^{-1} (CO stretching bend). Similar peaks observed for 6CFNvPNPs5 nanoparticles and 6CFP80NvPNPs5 nanoparticles indicates the entrapment of 6CF and compatibility with drug and excipients (Sarmento et al. 2006) (Fig. 2b). The FT-IR spectroscopy showed that the drug and excipients were free of any interaction and hence compatible.

Table 3 Physicochemical characterization of coated nanoparticles and 6CF-tagged nanoparticles. Data represented as mean ± SD, $n = 3$

Sr no.	Formulation	Mean particle size (nm) $n = 3$	PDI	Zeta potential (mV) $n = 3$	% EE $n = 3$	% DL $n = 3$
1	NvPNPs5	128.43 ± 4.82	0.283 ± 0.038	− 72.1 ± 0.00	39.50 ± 0.50	0.99 ± 0.01
2	P80NvPNPs5	218.3 ± 7.30	0.179 ± 0.00	− 16.2 ± 0.00	39.21 ± 0.05	0.975 ± 0.01
3	6CFNvPNPs5	187.5 ± 2.35	0.261 ± 0.08	− 16.2 ± 0.00	39.21 ± 0.05	0.975 ± 0.01
4	6CFP80NvPNPs5	259.9 ± 5.05	0.426 ± 0.19	− 13.6 ± 0.00	39.20 ± 0.05	0.975 ± 0.01

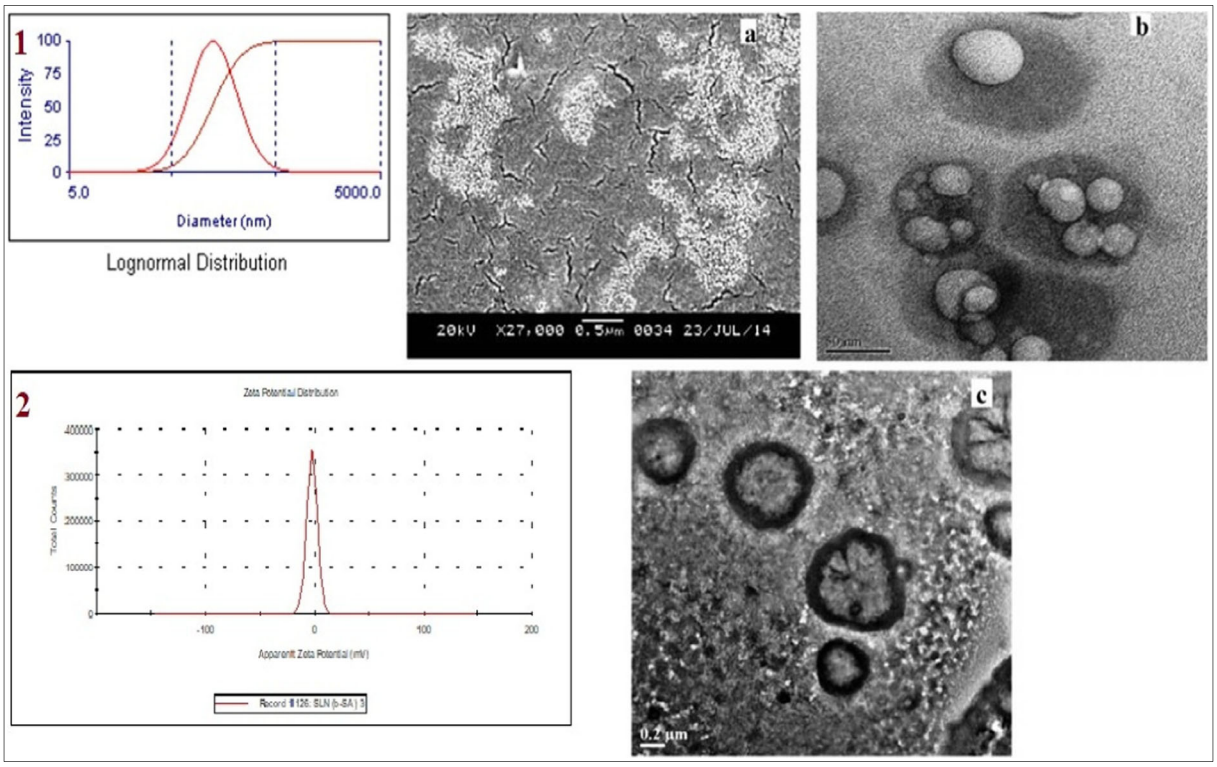

Fig.1 (1) Mean particle size (nm) of NvPNPs5, (2) zeta potential (mV) of NvPNPs5 shows sharp peak revealing stable nanoparticles, SEM of (a) NvPNPs5 shows small-sized spherical shaped nanoparticles, (b) TEM of NvPNPs5 shows small-sized spherical (≤ 50 nm) shaped nanoparticles, and (c) TEM of P80NvPNPs5 shows small-sized spherical shaped nanoparticles with the presence of coating layer

DSC

The illustration of DSC thermogram (Fig. 3a) explains the crystalline nature of NVP due to its sharp endothermic peak at 250.57 °C corresponding to its melting point. The DSC thermogram for NvPNPs5 and P80NvPNPs5 indicate the endothermic peaks at 54.01 °C and 51.77 °C respectively. The absence of NVP peak in the DSC thermogram of NvPNPs5 and P80NvPNPs5 was due to the entrapment of NVP, in an amorphous state (Fig. 3c, d) (Kumar et al. 2011). DSC showed that NVP and other excipients were compatible and free of interaction.

Morphology and surface characteristics

SEM

SEM of NvPNPs5 indicates uniform distribution and less aggregation of smaller sized (< 50 nm), spherical-shaped nanoparticles (Fig. 1a).

TEM

TEM of NvPNPs5 shows smaller sized (100 nm), spherical-shaped and smooth-surface nanoparticles (Fig. 1b). TEM of P80NvPNs5 also shows spherical shaped nanoparticles. The P80NvPNPs5 shows particle size of 100 to 200 nm which is greater than the uncoated nanoparticles, NvPNPs5. Also, the presence of PS80 coating on the surface of P80NvPNPs5 shows the adsorption of PS80 to nanoparticles surface (Fig. 1b, c). It is observed that the presence of hydrodynamic layer on the surface increased the mean particle size significantly when examined by particle size analyser than that of SEM, TEM (Table 3, Fig. 1).

Determination of the binding ratio of fluorescence marker/nevirapine

6CF shows good binding with NVP as no free fluorescent marker; 6CF was detected in the supernatant upon quantitative determination by Ultraviolet-Visible spectroscopy.

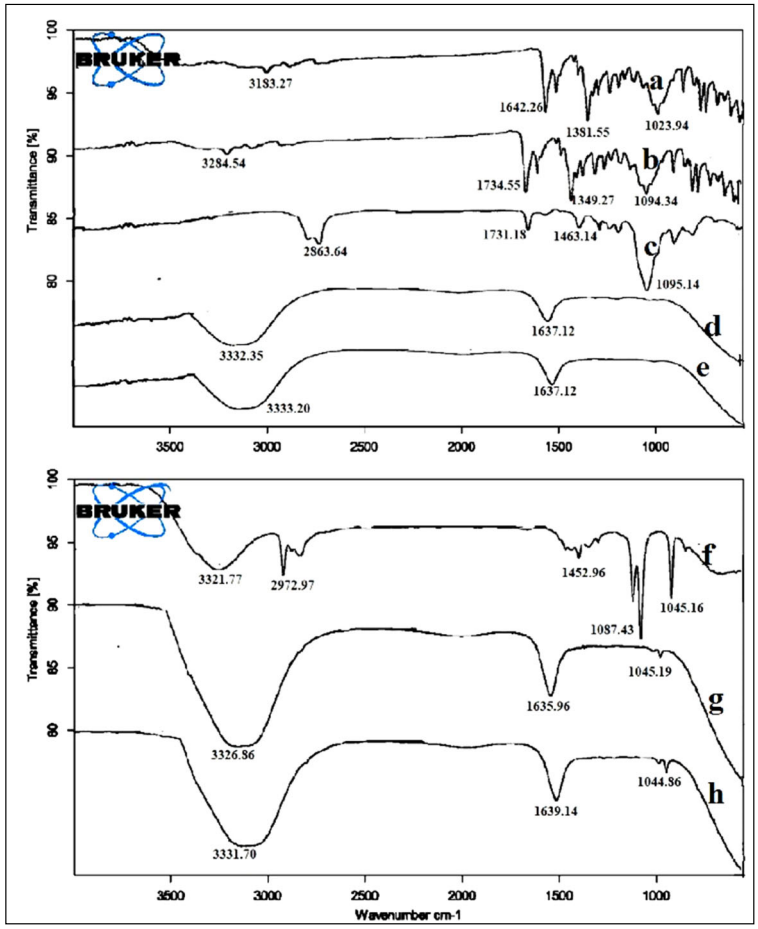

Fig. 2 FT-IR of (a) NVP, (b) PS80, (c) Physical mixture, (d) NvPNPs5, (e) P80NvPNPs5 nanoparticles, (f) 6CF, (g) 6CFNvPNPs5 nanoparticles, (h) 6CFP80NvPNPs5 nanoparticles. It reveals absence of drug excipients interaction

In vitro drug release study

P80NvPNPs5 nanoparticles could release (96.60 ± 2.11) % of drug, maintaining a sustained release effect for 36 h without any initial burst release as compared with NvPNPs5. NvPNPs5 and P80NvPNPs5 could release (83.00 ± 1.80) % and (42.11 ± 1.15) % of drug in 8 h respectively. NvPNPs5 could not release drug after 12 h, whereas free drug suspension showed an immediate drug release of (97.00 ± 0.00) % in 2 h (Fig. 4). The reason of slow drug release for P80NvPNPs5 nanoparticles was may be due to the surface coating; the hydrophobic regions of PS80 have strong adsorption properties for hydrophobic drug, thereby retarding the release of the drug to the dissolution media (Xiaojun et al. 2018). Both NvPNPs5 and P80NvPNPs5 nanoformulation were best fitted with Higuchi model, $R^2 = 0.979$ for NvPNPs5 and $R^2 = 0.936$ for P80NvPNPs5. P80NvPNPs5 drug release data inserted in Korsemeyer Peppas model showed anomalous non-Fickian drug release as $n = 0.767$ for $0.45 < n < 0.89$. While NvPNPs5, showed Super case II transport as value of $n > 0.89$, i.e. $n = 0.986$ (Table 4).

Stability studies

The nanoformulation was stable with slight variation in mean particle size and no significant change in the physical appearance, % EE, % DL when stored at refrigerated (5 ± 3 °C) and room temperature (25 ± 2 °C) for 120 days (Table 5).

Animal study

In vivo biodistribution study

The HPLC method of validation showed its linearity, specificity, accuracy and precision for quantitative determination of NVP. The obtained linear regression

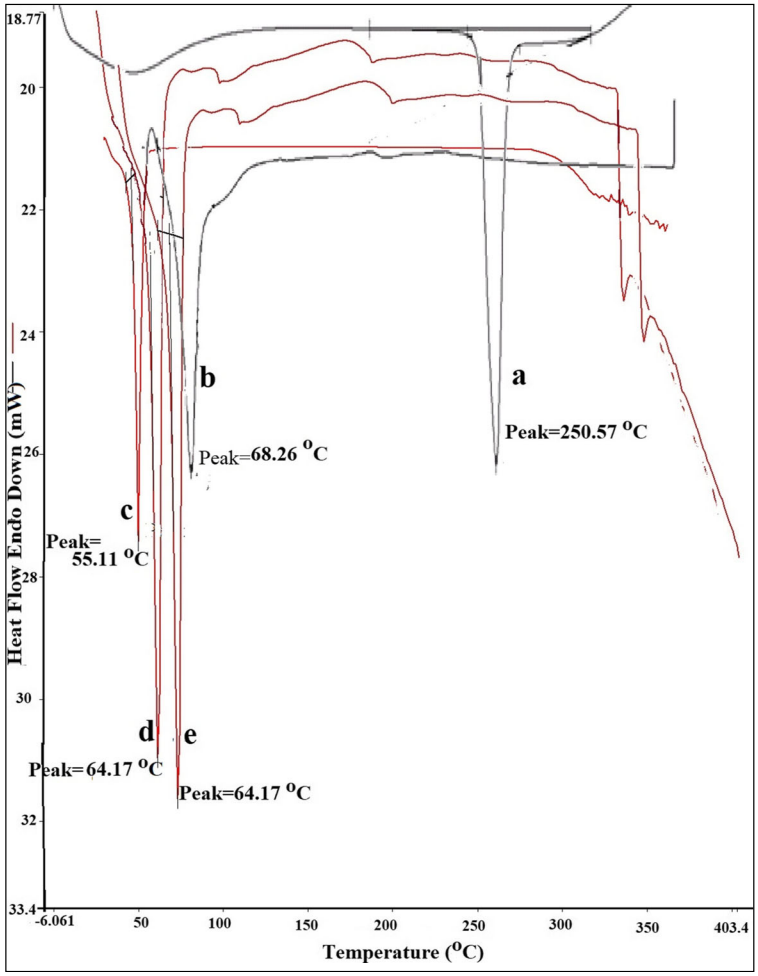

Fig. 3 DSC of (a) NVP, (b) PCL, (c) physical mixture, (d) NvPNPs5 and (e) P80NvPNPs5 shows absence of drug excipient interaction

equation, (Absorbance = 3.902 × Concentration + 2.207), R^2 = 0.953, showed its linearity in the range of 1 to 8 μg/ml. The specificity of HPLC method was accurate as no interfering peaks were found in the NVP chromatogram within retention time of 6.911 min (Fig. 5a, b). The precision of the method was accurate and reproducible. The recovery test showed accuracy of HPLC method, as percent recovery was found to be (100.01 ± 0.58) %. The LOD and LOQ was found to be (1.41 ± 0.78) μg/ml and (4.28 ± 2.37) μg/ml respectively. A lower LOD and LOQ value indicated sensitivity of the HPLC method. In vivo biodistribution study was carried out in Swiss Wistar rats in order to evaluate the ability of PCL nanoparticles to deliver NVP to the brain. The variation in the distribution of drugs in different organs and blood were determined quantitatively using HPLC (Fig. 5c, d). The concentration of drug in the brain when administered in P80NvPNPs5 nanoformulation was much higher than that of NvPNPs5 nanoformulation and free drug suspension post-injection through i.v. route (Figs. 5c and 6a). The P80NvPNPs5 nanoformulation released (2.231 ± 0.005) μg/g drug in the brain after 24 h of post-injection. Whereas NvPNPs5 nanoformulation could release (0.588 ± 0.001) μg/g of drug in the brain after 6 h post-injection. No drug was detected in the brain after 24 h post-injection when administered with NvPNPs5 nanoformulation. On the other hand no drug was detected in the brain when administered in the form of free NVP suspension (Fig. 6a) (Christoper et al. 2014; Wilson et al. 2008). In blood serum, the concentration of drug when administered with P80NvPNPs5 nanoformulation was much higher than the NvPNPs5 nanoformulation and free NVP suspension (Figs. 5c, d and 6b). The P80NvPNPs5 nanoformulation was able to release the drug for 48 h. P80NvPNPs5 showed (4.008 ± 0.006) μg/ml of drug after 24 h of post-injection. P80NvPNPs5 nanoparticles could

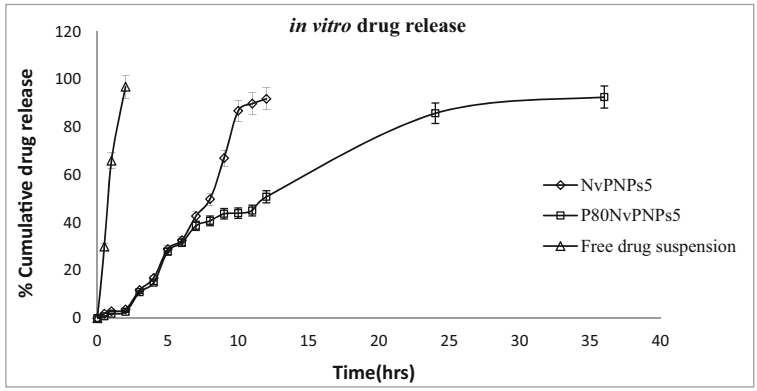

Fig. 4 In vitro drug release study (mean ± SD, $n = 3$) shows that NvPNPs5 released NVP for 8 h and P80NvPNPs5 showed sustained release of NVP for 36 h

maintain a prolonged blood circulation for 48 h and a drug concentration of (0.800 ± 0.001) μg/ml was detected in blood serum even after 48 h of post-injection. Whereas, NvPNPs5 showed (0.600 ± 0.001) μg/ml of drug in the blood serum after 24 h post injection. Free drug suspension showed (0.600 ± 0.001) μg/ml of drug in the blood after 6 h of post-injection. While free drug suspension showed no drug was in blood after 24 h post-injection (Fig. 6b). Moreover, the drug distribution was also found in other organs—liver, spleen, kidney. The drug distribution in these organs after post-injection at different time intervals of 1 h, 2 h, 4 h, 6 h and 24 h are shown in Fig. 5c and d. The drug accumulated to a lesser extent in liver and spleen when administered with P80NvPNPs5 nanoformulation, whereas, greater extent of drug accumulated in these organs when administered in the form of NvPNPs5 nanoformulation. The lesser accumulation of drug with P80NvPNPs5 nanoparticles may be due to the presence of PS80 coating layer which imparts hydrophilicity and avoids the RES in blood, preventing the phagocytosis by MPS organs like liver and spleen (Goppert and Muller 2005; Alyautdin et al. 1997). A lesser extent of drug accumulated in the kidney when administered with P80NvPNPs5 than that of NvPNPs5 nanoformulation and free drug suspension due to the decrease in clearance and increase in half-life ($t_{1/2}$) of the drug (Table 6). The stable nanoparticles as determined by zeta potential analysis and stability studies indicate that the P80NvPNPs5 nanoformulation had a longer stay in blood circulation with an increase in the $t_{1/2}$, (24.97 ± 0.01) h which is higher than the NvPNPs5 nanoformulation, (7.28 ± 0.02) h and free drug suspension, (3.32 ± 0.02) h. The minimum therapeutic concentration of NVP is reported to be 3 μg/ml (Kimulwo et al. 2017). In brain, P80NvPNPs5 could release (3.39 ± 0.02) μg/ml of NVP at (1.00 ± 0.00) h (Lamorde et al. 2011). So, NVP loaded in P80NvPNPs5 was able to attain minimum therapeutic concentration at (1.00 ± 0.00) h. The drug in P80NvPNPs5 showed maximum concentration (C_{max}) of (5.88 ± 0.03) μg/ml at (4.00 ± 0.00) h (T_{max}). A higher concentration of drug in the brain and blood was attained with P80NvPNPs5 nanoformulation in comparison with NvPNPs5 nanoformulation and a plain drug suspension. The longer stay of P80NvPNPs5 nanoparticles in blood having mean residence time $MRT_{0\ to\ t}$ of (16.91 ± 0.01) h increases the penetration of nanoparticles in the brain which increases the bioavailability of drug in the brain. P80NvPNPs5 nanoparticles showed $MRT_{0\ to\ t}$ of (9.54 ±

Table 4 Mechanism of drug release kinetics

Formulation code	Zero-order drug release model		First-order drug release model		Higuchi drug release model		Hixson-Crowelldrug release model		Korsemeyer Peppas model	
	R^2	K_0(mg ml^{-1} min^{-1})	R^2	K_1(min^{-1})	R^2	K_H(mg ml^{-1} min^{-1})	R^2	K_{HC}(mg ml^{-1} min^{-1})	R^2	n
NvPNPs5	0.933	0.159	0.856	−0.016	0.979	2.42	0.809	0.24	0.972	0.986
P80NvPNPs5	0.752	2.560	0.928	−0.059	0.936	18.64	0.752	0.085	0.906	0.767

R^2 is the correlation coefficient; K_0, K_1, K_H, K_{HC} are the release rate constant for Zero-order, First-order, Higuchi and Hixson-Crowell drug release model. n represents release exponent for Korsemeyer Peppas model

Table 5 Stability studies, mean ± SD, $n = 3$

Storage time/Physico. char.	NvPNPs5					P80NvPNPs5				
	0 day	30 days	60 days	90 days	120 days	0 day	30 days	60 days	90 days	120 days
At 5 ± 3 °C										
Mean particle size (nm)	123.2 ± 3.1	123.2 ± 2.1	124.3 ± 3.6	124.4 ± 3.5	124.4 ± 3.6	209.3 ± 4.7	209.3 ± 4.4	209.3 ± 4.7	209.3 ± 4.6	209.3 ± 4.5
Zeta potential (mV)	− 72.1 ± 0.2	− 72.1 ± 0.2	− 72.1 ± 0.2	− 72.1 ± 0.2	− 72.1 ± 0.2	− 16.2 ± 0.2	− 16.2 ± 0.2	− 16.2 ± 0.2	− 16.2 ± 0.2	− 16.2 ± 0.2
% EE	39.54 ± 0.08	39.34 ± 0.08	39.34 ± 0.03	39.14 ± 0.09	39.34 ± 1.08	39.21 ± 0.05	39.51 ± 1.01	39.81 ± 1.02	39.81 ± 0.8	39.91 ± 0.8
% DL	0.976 ± 0.06	0.976 ± 0.04	0.978 ± 0.08	0.976 ± 0.03	0.978 ± 0.06	0.976 ± 0.07	0.975 ± 0.06	0.975 ± 0.08	0.945 ± 0.07	0.985 ± 0.05
Physical appearance	No significant change	No significant change	No significant change	No significant change	No significant change	No significant change	No significant change	No significant change	No significant change	No significant change
At 5 ± 3 °C										
Mean particle size (nm)	123.2 ± 3.1	123.2 ± 2.1	124.3 ± 3.6	124.4 ± 3.5	124.4 ± 3.6	209.3 ± 4.7	209.3 ± 4.4	209.3 ± 4.7	209.3 ± 4.6	209.3 ± 4.5
Zeta potential (mV)	− 72.1 ± 0.1	− 72.1 ± 0.2	− 72.1 ± 0.2	− 72.1 ± 0.2	− 72.1 ± 0.2	− 16.2 ± 0.2	− 16.2 ± 0.2	− 16.2 ± 0.2	− 16.2 ± 0.2	− 16.2 ± 0.2
% EE	39.54 ± 0.08	39.34 ± 0.08	39.34 ± 0.03	39.14 ± 0.09	39.34 ± 1.08	39.21 ± 0.05	39.51 ± 1.01	39.81 ± 1.02	39.81 ± 0.8	39.91 ± 0.8
% DL	0.975 ± 0.06	0.976 ± 0.01	0.978 ± 0.05	0.976 ± 0.06	0.978 ± 0.06	0.976 ± 0.07	0.975 ± 0.06	0.975 ± 0.08	0.945 ± 0.07	0.985 ± 0.05
Physical appearance	No significant change	No significant change	No significant change	No significant change	No significant change	No significant change	No significant change	No significant change	No significant change	No significant change

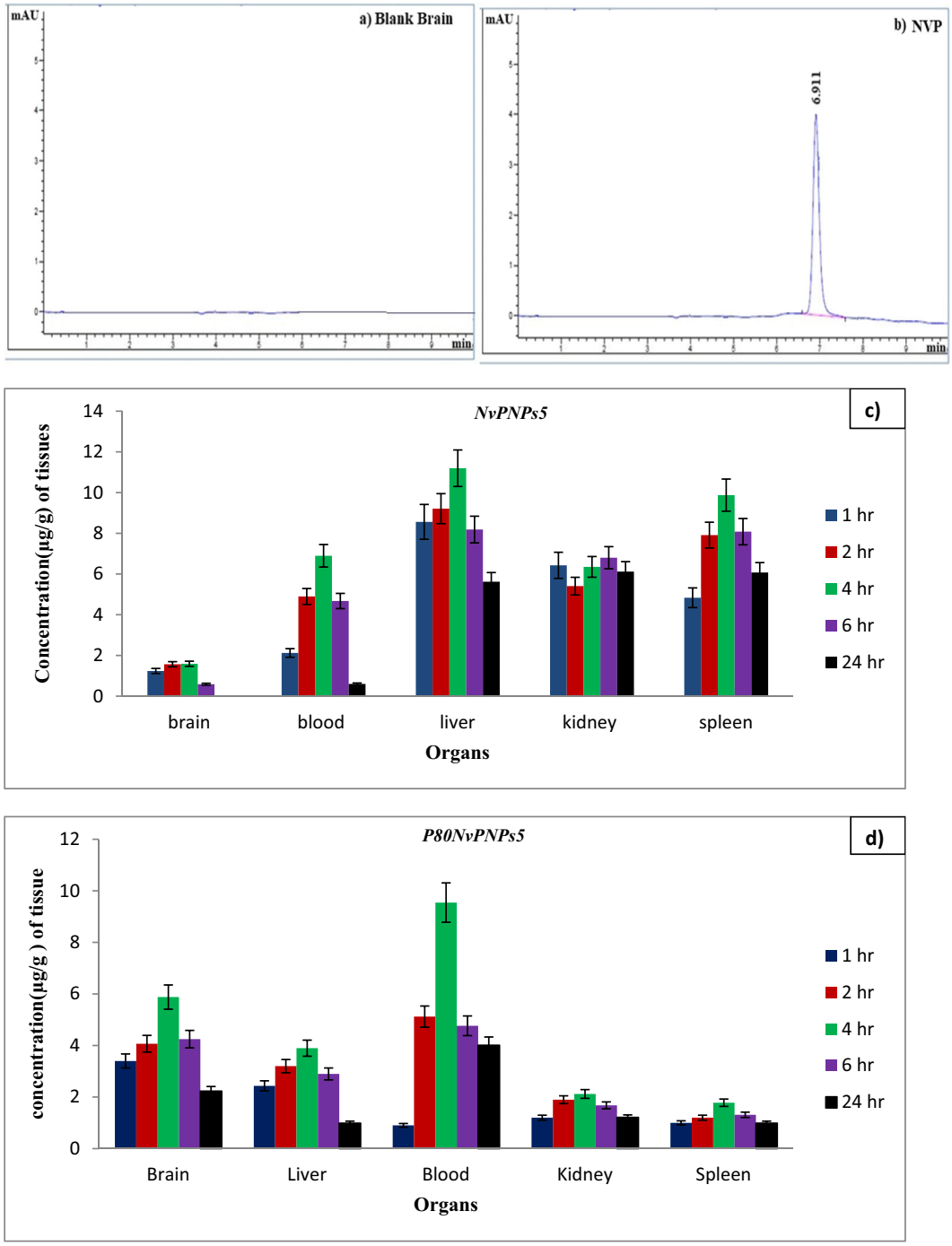

Fig. 5 (a) HPLC chromatogram of blank brain, (b) HPLC chromatogram of NVP. Biodistribution of nanoparticles in different organs at different time interval, (c) NvPNPs5 and (d) P80NvPNPs5 nanoparticles indicates that P80NvPNPs5 could release higher concentration of NVP in blood and brain than NvPNPs5. P80NvPNPs5 reduced nonspecific accumulation in other nonspecific organs like liver, kidney and spleen. Mean ± SD, $n = 3$

0.12) h, $t_{1/2}$ of (24.57 ± 0.01) h in the brain. It is observed from the study that P80NvPNPs5 nanoparticles could easily cross the blood-brain barrier than that of NvPNPs5 nanoparticles and a free drug suspension. P80NvPNPs5 nanoparticles may act on the Low-density lipoprotein (LDL) receptors found in the luminal membrane of

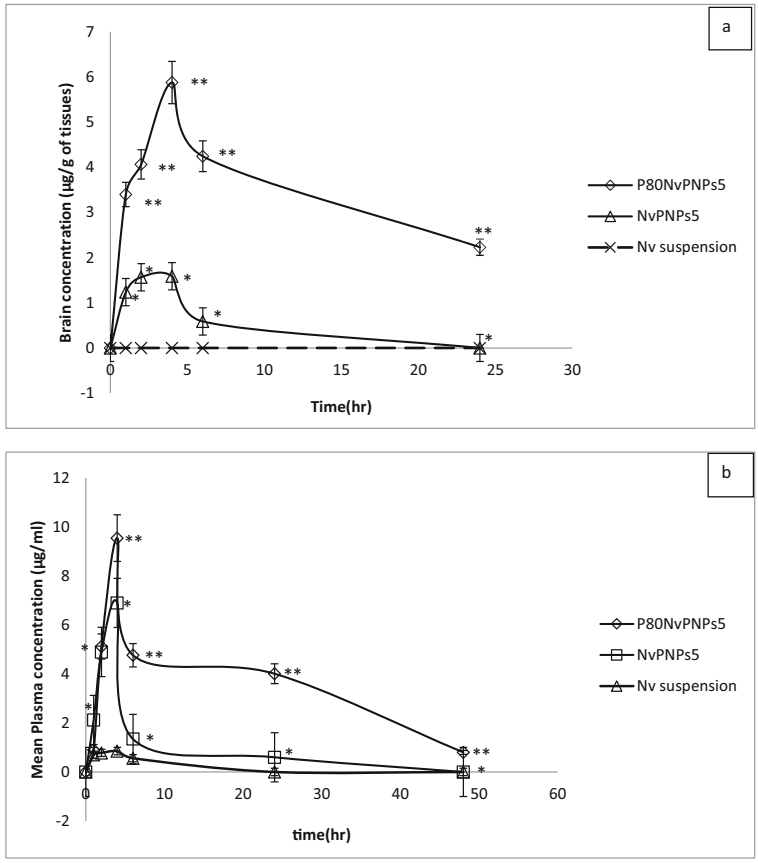

Fig. 6 Concentration of drug in (a) brain concentration (μg/g) after i.v. administration of free NVP suspension, NvPNPs5 and P80NvPNPs5 at a dose of 20 mg/kg. (b) Mean plasma concentration (μg/ml) after i.v. administration of free NVP suspension, NvPNPs5 and P80NvPNPs5 at a dose of 20 mg/kg. Mean ± SD, $n = 3$. *$p < 0.05$, NvPNPs5 compared with free NVP suspension (Tukey's test, one-way ANOVA) and **$p < 0.05$ P80NvPNPs5 compared with NvPNPs5 (Tukey's test, one way ANOVA)

BCECs and penetrates through the BCECs by receptor-mediated endocytosis. All these results signify that P80NvPNPs5 nanoparticles could efficiently target NVP to the brain. It also reduced the nonspecific accumulation of the drug in other nonspecific organs reducing the possibility of undesirable side effects and toxic effects. ANOVA (Tukey's test, one way ANOVA) shows that the obtained data were statistically significant at $p < 0.05$ (Fig. 6a, b).

CLSM

The coated nanoparticles targeted to the rat brain were identified at the cellular level (Fig. 7a1 to e3). The blue

Table 6 Pharmacokinetic parameters of nanoparticles in brain and blood serum

Pharmacokinetic parameters of nevirapine polycaprolactone nanoparticle								
	Nanoformulation	C_{max} (μg g^{-1})	T_{max} (h)	$AUC_{(10-t)}$ (μg min g^{-1})	$t_{1/2}$ (h)	CL (ml h^{-1})	V_d (ml)	$MRT_{0\ to\ t}$ (h)
Brain	P80NvPNPs5	1.59 ± 0.03	4.00 ± 0.00	83.81 ± 0.05	24.57 ± 0.01	0.12 ± 0.00	4.35 ± 0.10	9.54 ± 0.12
	NvPNPs5	1.59 ± 0.02	4.00 ± 0.00	12.64 ± 0.06	2.83 ± 0.05	1.58 ± 0.00	6.45 ± 0.20	4.26 ± 0.12
Blood	P80NvPNPs5	9.54 ± 0.03	4.00 ± 0.00	169.11 ± 0.05	24.97 ± 0.01	0.10 ± 0.00	3.64 ± 0.02	16.91 ± 0.01
	NvPNPs5	6.90 ± 0.03	4.00 ± 0.00	49.31 ± 0.02	7.28 ± 0.02	0.41 ± 0.00	4.26 ± 0.02	9.23 ± 0.10
	Pure drug	0.85 ± 0.01	4.00 ± 0.00	9.17 ± 0.03	3.32 ± 0.02	2.18 ± 0.00	10.45 ± 0.02	4.74 ± 0.02

Mean ± SD, $n = 3$

C_{max} peak plasma concentration, T_{max} time to reach peak plasma concentration, AUC area under the curve, $MRT_{0\ to\ t}$ mean residence time

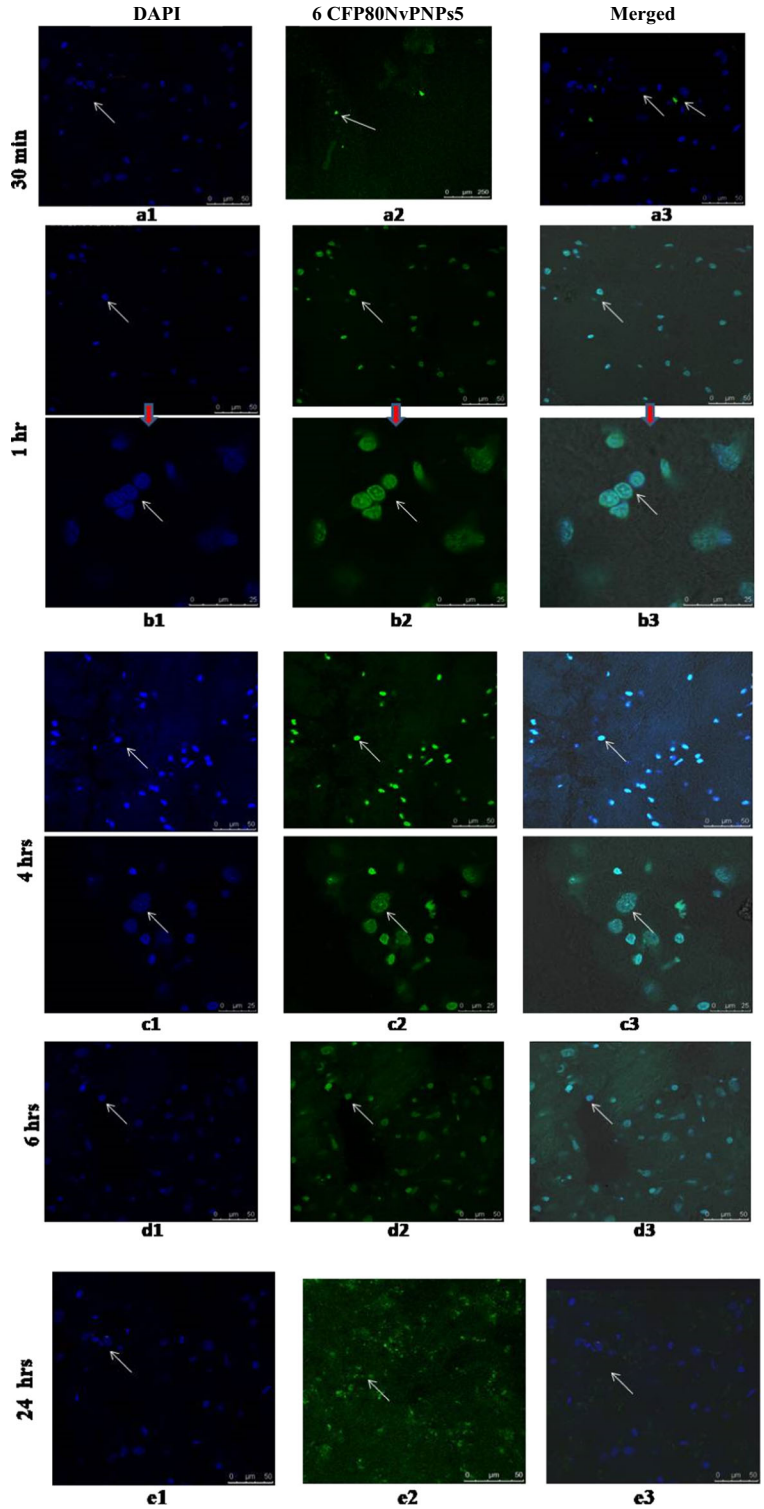

Fig. 7 Distribution of 6CFP80NvPNPs5 nanoparticles in cryosectioned Wistar rat brain tissues at different time interval shows highest fluorescence intensity at 4 h. The fluorescence intensity could be seen even after 24 h post-injection

colour fluorescence (DAPI stained) indicates brain tissues whereas green fluorescence indicates the 6CFP80NvPNPs5 nanoparticles. After 30 min, the 6CFP80NvPNPs5 nanoparticles were present surrounding the brain tissues (Fig. 7a1 to a3). One hour after administration, the fluorescence had started to spread throughout the brain tissues. The fluorescence was observed in the capillary lumen, brain endothelial cells and perivascular tissues (Fig. 7b1 to b3).

It was hypothesized that PS80-coated nanoparticles, P80NvPNPs5 adsorbed Apolipoprotein, especially ApoE and ApoB, present in the bloodstreams mimic lipoprotein particles which could interact with the low-density lipoprotein receptors (LDLr) and were taken up by the brain capillary endothelial cells via receptor-mediated endocytosis. Then the drug might be released in these cells and diffused into the brain interior or the particles might be transcytosed (Jones and Shusta 2007; Masserini 2013;Garcia et al. 2005) (Fig. 7b1 to d3). Other hypothesis suggests that an increased retention of nanoparticles in the brain blood capillaries and binding to endothelial cell lining could provide a drug concentration gradient and thus enhanced drug transport across the blood-brain barrier by passive diffusion (Kreuter 2001). Inhibition of drug efflux transporters especially P-gp at the blood-brain barrier is also an approach that provides improved internalization of P-gp substrates into the brain (Chen and Liu 2012). Based on the surfactant effect, it might be characterized by solubilization of the endothelial cell membrane lipids that would lead to membrane fluidization and destabilization and enhanced drug permeability through the blood-brain barrier (Wang et al. 2013).

In addition, P80NvPNPs5 nanoparticles underwent prolonged circulation in the blood bypassing RES phagocytosis. This characteristic is required for targeting specific site so as to release sufficient concentration of drug within its therapeutic range (Chang et al. 2009; Ambruosi et al. 2006; Petri et al. 2007). A less intense fluorescence was detected with 6CFP80NvPNPs5 nanoparticles in brain tissues at 30 min with a gradual increase in intensity. 6CFP80NvPNPs5 showed the highest fluorescence intensity in 4 h. After that, there is a gradual decrease in fluorescence intensity upto 6 h. A very less fluorescence intensity was detected in brain tissues after 24 h post injection (Fig. 7e1 to e3). This result acts in accordance with the in vivo biodistribution study in brain, where the maximum drug concentration in the brain was detected in 4 h. Thus, this study shows an adequate distribution of 6CFP80NvPNPs5 in the brain tissues which is needed to achieve sufficient concentration of NVP within its therapeutic range. As such, maintenance of NVP within therapeutic range improves its bioavailability. Also, detection of 6CFP80NvPNPs5 in brain tissues even after 24 h post-injection supports the results of in vivo Biodistribution study because P80NvPNPs5 showed (2.231 ± 0.005) μg/g NVP in brain after 24 h of post-injection. So, 6CFP80NvPNPs5 showed sustained release of NVP in brain.

Conclusion

The present study systematically describes the biodistribution and efficacy of PS80-coated PCL nanoparticles to deliver NVP across the blood-brain barrier. The result showed that the drug, NVP could be easily targeted to the brain when incorporated in PS80-coated nanoparticles. The coated nanoparticles penetrate the BCECs by receptor-mediated endocytosis into the brain parenchyma. It can be concluded that PS80 has a futuristic scope as a coating material to formulate drug delivery system for efficiently targeting the drugs to the brain.

Acknowledgements The authors express their obliged acknowledgment to Dibrugarh University for technical support; GIPS, Guwahati, for particle size analysis and FT-IR spectroscopy; IASST, Guwahati, for allowing availing DSC and zeta Potential analysis. We are also thankful to SAIF, NEHU, Shillong, for helping us with SEM and TEM analysis; Guwahati Biotech Park, IIT Guwahati, for permitting CLSM study and College of Veterinary Sciences, AAU, Guwahati, for animal studies.

Compliance with ethical standards Animal studies were performed with the permission of the Institutional Animal Ethics Committee (IAEC) of Dibrugarh University, Assam, India. All the institutional and national guidelines for the care and use of laboratory animals were followed.

Conflict of interest The authors declare that they have no conflict of interest.

References

Acharya SR, Reddy PRV (2016) Brain targeted delivery of paclitaxel using endogenous ligands. Asian J Pharm Sci 11:427–438

Alyautdin RN, Petrov VE, Langer K, Berthold A, Kharkevich DA, Kreuter J (1997) Delivery of loperamide across the blood-brain barrier with polysorbate80 coated polybutylcyanoacrylate nanoparticles. Pharm Res 14:325328

Ambruosi A, Khalansky AS, Yamamoto H, Gelperina SE, Begley DJ, Kreuter J (2006) Biodistribution of Polysorbate 80 coated doxorubicin loaded [14C]-poly(butyl cyanoacrylate) nanoparticles after intravenous administration to Glioblastoma-bearing rats. J Drug Target 14:97–105

Azimi B, Nourpanah P, Rabiee M, Arbab S (2014) Poly (ε-caprolactone) fiber: an overview. J Eng Fibers Fabrics 9: 74–90

Badri W, Miladi K, Robin S, Viennet C, Nazari QA, Agusti G, Fessi H, Elaissari A (2017) Polycaprolactone based nanoparticles loaded with indomethacin for anti-inflammatory therapy: from preparation to ex vivo study. Pharm Res 34:1773–1783

Banker GS, Anderson NR (1990) Tablets. In: The theory and practice of Industrial pharmacy, 3rd (Edition) edn. Varghese Publishing House, Dadar, Bombay, India, pp 293–345

Bohn KA, Adkins CE, Mittapalli RK, Terell-Hall TB, Mohammad AS, Shah N et al (2016) Semi-automated rapid quantification of brain vessel density utilizing fluorescent microscopy. J Neurosci Methods 270:124–131

Bondi ML, Craparo EF, Giammona G, Drago E (2010) Brain–targeted solid lipid nanoparticles containing Riluzole: preparation, characterization and biodistribution. Nanomed 5:25–32

Campos EVR, Oliveira JLD, Silva CMGD, Pascoli M, Pasquoto T, Lima R (2015) Polymeric and solid lipid nanoparticles for sustained release of Carbendazim and Tebuconazole in agricultural applications. Sci Rep 5:13809

Chacko BJ, Palanisamy S, Gowrishankar NL, Honeypriya J, Sumathy A (2018) Effect of surfactant coating on brain targeting polymeric nanoparticles; a review. Indian J Pharm Sci 80:215–222

Chang J, Jallouli J, Kroubi M, Yuan XB, Feng W, Kang CH et al (2009) Characterisation of endocytosis of transferrin coated PLGA nanoparticles by the blood-brain barrier. Int J Pharm 379:285–292

Chen Y, Liu L (2012) Modern methods for delivery of drugs across the blood-brain barrier. Adv Drug Deliv Rev 64: 640–665

Choi SW, Kim WS, Kim JH (2003) Surface modification of functional nanoparticles for controlled drug delivery. J Dispers Sci Technol 24:475–485

Christoper GVP, Raghavan CV, Siddharth K, Kumar MSS, Prasad RH (2014) Formulation and optimization of coated PLGA–Zidovudine nanoparticles using factorial design and *in vitro in vivo* evaluations to determine brain targeting efficiency. Saudi Pharm J 22:133–140

Daneman R, Prat A (2015) The blood-brain barrier. CHS Perspect Biol 7:020412

Dash S, Murthy PN, Nath LK, Choudhury P (2010) Kinetic modeling on drug release from controlled drug delivery systems. Acta Pol Pharm Drug Res 67(3):217–223

Dora CP, Singh SK, Kumar S, Datusalia AK, Deep A (2010) Development and characterization of nanoparticles of Glibenclamide by solvent displacement method. Acta Pol Pharm Drug Res 67:283–290

Garcia EG, Andrieux K, Gil S, Couvreur P (2005) Colloidal carriers and blood-brain barrier (BBB) translocation: a way to deliver drugs to the brain? Int J Pharm 298:274–292

Ghaly ES, Sastre V (2014) Controlled release of ibuprofen nanoparticles: Physico-chemical characterization and drug release. Int J Pharm Pharm Sci 6:99–107

Goppert TM, Muller RH (2005) Polysorbate-stabilized solid lipid nanoparticles as colloidal carriers for intravenous targeting of drugs to the brain: Comparision of plasma protein adsorption pattern. J Drug Target 13:179–187

Hague S, Md S, Sahni JK, Ali J, Baboota S (2014) Development and evaluation of brain-targeted intranasal alginate nanoparticles for treatment of depression. J Psychiatr Res 48:1–12

Honary S, Zahir F (2013) Effect of zeta potential on the properties of Nano-drug delivery systems - a review (part 1). Trop J Pharm Res 12:255–264

Jia Y, Ji J, Wang F, Shi L, Yu J, Wang D (2016) Formulation, characterization and *in-vitro/vivo* study of Aclacinomycin a loaded solid lipid nanoparticles. Drug Deliv 23:1317–1325

Jones AR, Shusta EV (2007) Blood-brain barrier transport of therapeutics via receptor-mediation. Pharm Res 24:1759–1771

Kaur A, Jain S, Tiwary AK (2008) Mannan coated gelatin nanoparticles for sustained and targeted delivery of Didanosine: *in-vitro* and *in-vivo* evaluation. Acta Pharma 58:61–74

Kimulwo MJ, Okendo J, Ochieng W (2017) Plasma Nevirapine concentrations predict virological and adherence failure in Kenyan HIV-1 infected patients with extensive antiretroviral treatment exposure. PLoS One 12(2):1–14

Kreuter J (2001) Nanoparticulate systems for brain delivery of drugs. Adv Drug Deliv Rev 47:65–81

Ku S, Yan F, Wang Y, Sun Y, Yang N, Ye L (2010) The blood-brain barrier penetration and distribution of PEGylated fluorescein-doped magnetic silica nanoparticles in rat brain. Biochem Biophys Res Commun 394:871–876

Kumar P, Mohan C, Uma Shankar MKS, Gulati M (2011) Physiochemical characterization and release rate studies of solid dispersions of ketoconazole with Pluronic F127 and PVP K-30. Ir J Pharm Res 10:685–694

Kuo YC, Lin PI, Wang CC (2011) Targeting Nevirapine delivery across human brain microvascular endothelial cells using transferrin–grafted poly (lactide-co-glycolide). Nanomedicine (London) 6(6):1011–1026

Lahkar S, Das MK (2017) Effects of solvents on the development of biodegradable polymeric nanoparticles of Nevirapine. Int J ChemTech Res 10:735–747

Lahkar S, Das MK (2018) Surface modified kokum butter lipid nanoparticles for the brain targeted delivery of Nevirapine. J Microencapsul 35(7–8):680–694

Lajoie JM, Shusta EV (2015) Targeting receptor-mediated transport for delivery of biologics across the blood-brain barrier. Annu Rev Pharmacol Toxicol 55:613–631

Lamorde M, Kibwika PB, Merry C (2011) Nevirapine pharmacokinetics when initiated at 200 mg or 400 mg daily in HIV-1 and tuberculosis co-infected Ugandan adults on rifampicin. J Antimicrob Chemother 66(1):180–183

Masserini M (2013) Nanoparticles for brain drug delivery. ISRN Biochem 2013:238428

Nevirapine (2007) Indian Pharmacoepia, vol 3, 5th edn. Indian Pharmacopoeia Commision, Ghaziabad, India, pp 819–820

Pal SL, Jana U, Manna PK, Mohanta GP, Manavalan R (2011) Nanoparticle: an overview of preparation and characterization. J Appl Pharm Sci 6:228–234

Pardridge WM (2005) The blood-brain barrier: bottleneck in brain drug development. NeuroRx 2:3–14

Parikh T, Bommana MM, Squillante E (2010) Efficacy of surface charge in targeting pegylated nanoparticles of Sulpiride to the brain. Eur J Pharm Biopharm 74:442–450

Patil VC, Patil HC (2014) Neurological manifestations of HIV-AIDS at a tertiary care center in western Maharashtra. Int J Med Pub Health 4:210–217

Petri B, Bootz A, Khalansky A, Hekmatara T, Muller R, Uhl R, Kreuter J, Gelperina S (2007) Chemotherapy of a braintumor using doxorubicin bound to surfactant-coated poly (butyl cyanoacrylate) nanoparticles: revisiting the role of surfactants. J Control Release 117:51–58

Phosphate buffer, pH 7.4 (1996) Indian Pharmacopoeia. Indian Pharmacopoeia Commision, Ghaziabad

Ramanujam R, Sundaram B, Janarthanan G, Devendran E, Venkadasalam M, John Milton MC (2018) Biodegradable Polycaprolactone nanoparticles based drug delivery systems: a short review. Biosci Biotech Res Asia 15:679–685

Ravisankar P, Navya CN, Pravallika D, Sri DN (2015) A review on step-by-step analytical method validation. IOSR J Pharm 5(10):07–19

Reimold I, Domke D, Bender J, Seyfried CA, Radunz HE, Fricker G (2008) Delivery of nanoparticles to the brain detected by fluorescence microscopy. Eur J Pharm Biopharm 70:627–632

Sabin CA, Lundgren HD (2013) The natural history of HIV infection. Curr Opin HIV AIDS 8(4):311–317

Saksena NK, Smit TK (2005) HAART & the molecular biology of AIDS dementia complex. Indian J Med Res 121:256–269

Salmaso S, Caliceti P (2013) Stealth properties to improve therapeutic efficacy of drug nanocarriers. J Drug Deliv 2013:1–20

Saraiva C, Praça C, Ferreira R, Santos T, Ferreira L, Bernardino L (2016) Nanoparticle-mediated brain drug delivery: overcoming blood-brain barrier to treat neurodegenerative diseases. J Control Release 235:34–47

Sarmento B, Ferreira D, Veiga F, Ribeiro A (2006) Characterization of insulin-loaded alginate nanoparticles produced by Ionotropic pre-gelation through DSC and FTIR studies. Carbohydr Polym 66:1–7

Souza SD (2014) A review of *in vitro* drug release test methods for nano-sized dosage forms. Adv Pharm 2014:1–12

Storm G, Belliot SO, Daemen T, Lasic DD (1995) Surface modification of nanoparticles to oppose uptake by the mononuclear phagocyte system. Adv Drug Deliv Rev 17:31–48

Sun W, Xie C, Wang H, Hu Y (2004) Specific role of Polysorbate 80 coating on the targeting of nanoparticles to the brain. Biomat 25:3065–3071

Tan IL, McArthur JC (2012) HIV-associated neurological disorders. CNS Drugs 26:123–134

Tian XH, Lin XN, Wei F, Feng W, Huang ZC, Peng W et al (2011) Enhanced brain targeting of Temozolamide in Polysorbate 80 coated polybutylcyanoacrylate nanoparticles. Int J Nanomedicine 6:445–452

Usach I, Melis V, Peris JE (2013) Non-nucleoside reverse transcriptase inhibitors: a review on pharmacokinetics, pharmacodynamics, safety, and tolerability. J Int AIDS Soc 16:1–14

Wang H, Jia Y, Hu JH, Zhang J, Zhang L (2013) Effect of preparation conditions on the size and encapsulation properties of mPEG-PLGA nanoparticles simultaneously loaded with vincristine sulfate and Curcumin. Pharm Dev Technol 18:694–700

Wilson B, Samanta MK, Santhi K, Kumar KPS, Paramakrishnan N, Suresh B (2008) Poly (n-butyl cyanoacrylate) nanoparticles coated with Polysorbate 80 for the targeted delivery of Rivastigmine to the brain to treat Alzheimer disease. Brain Res 1200:159–168

Wong AD, Ye M, Levy AF, Rothstein JD, Bergles DE, Searson PC (2013) The blood-brain barrier: an engineering perspective. Front Neuroeng 6:1–2

Xiaojun T, Yu L, Qian H, Li Z, Zixuan H, Jiajin Y, Xiaoping Y, Jianzhuo H, Xing F (2018) Preparation and drug release study of novel nanopharmaceuticals with Polysorbate 80 surface adsorption. J Nanomater 2018: 1–11

Yadav M, Parle M, Sharma N, Dhingra S, Raina N, Jindal DK (2017) Brain targeted oral delivery of doxycycline hydrochloride encapsulated tween 80 coated chitosan nanoparticles against ketamine-induced psychosis: behavioral, biochemical, neurochemical and histological alterations in mice. Drug Deliv 24:1429–1440